

Measurements of wave-cloud microphysical properties with two new aircraft probes

H. Gerber

Gerber Scientific Inc., 1643 Bentana Way, Reston, VA 20190

Cynthia H. Twohy, Bruce Gandrud, Andrew J. Heymsfield, Greg M. McFarquhar

National Center for Atmospheric Research, P.O. Box 3000, Boulder, CO 80307

Paul J. DeMott, David C. Rogers

Colorado State University, Fort Collins, CO 80523

Abstract. Measurements of ice water content (IWC) and mean ice-crystal size and concentration made by two *in-situ* probes, CVI and PVM, were compared on the DC-8 aircraft during SUCCESS flights in orographic ice clouds. The comparison of IWC in these wave clouds, that formed at temperatures of about -38°C on April 30 and -62°C on May 2, 1996, showed good agreement. The comparison of ice crystal concentrations agreed better for the April-30 clouds than for the May-2 clouds; and the effective radius compared for both probes and for remote retrievals from aircraft and satellite for a segment of the Berthoud wave cloud (May 2) agreed within 30%. The measured parameters of the ice crystals were similar to earlier measurements and recent modeling of cold wave clouds.

Introduction

The flights of the NASA Ames DC-8 research aircraft during the SUCCESS program in May - June, 1996 provided an opportunity for comparing the performance of new versions of two probes for measuring properties of ice crystals encountered in upper-tropospheric cirrus and contrail clouds. The probes, a CVI [counterflow virtual impactor; Noone et al. (1988); Ström and Heintzenberg (1994); Twohy et al. (1997)] and a PVM [particulate volume monitor; Gerber et al. (1994)], operate according to different physical principles, with the former evaporating the ice crystals and measuring the quantity of resulting water vapor with a Lyman- α hygrometer, and the latter measuring the crystals optically. However, both are expected to give similar results, because they are designed to measure similar ice-crystal properties. These properties include a measure of IWC (ice water content: total mass of ice per cloud volume), and estimates of a characteristic crystal size (R_v , mean volume radius for the CVI; and R_e , effective radius for the PVM) and N (number of ice crystals per unit cloud volume).

The comparisons described here between the two probes are limited to the DC-8 flights on April 30 and May 2 when the aircraft flew through orographic wave clouds. These cold clouds were expected to contain small and nearly spherical ice crystals, as found in earlier work on similar clouds (Heymsfield and Miloshevich, 1993, 1995; Ström et al., 1996); also the size range of the crystals was expected to be within the range of both probes, which is limited to a diameter of about $50\ \mu\text{m}$ for the PVM. The PVM is in addition sensitive to ice-crystal shape (Gerber et al., 1995). The CVI and PVM were mounted next to each other on the DC-8 fuselage in order to minimize the influence of the spatial variability of ice crystals on the comparison of the probes.

This paper addresses the question: How well do the PVM and CVI agree in measuring IWC, R_e , and N of the ice crystals?

Comparisons

Ice Water Content

The DC-8 flew through each wave cloud within a matter of minutes, because the clouds were limited in extent and generally isolated from each other. The distances the aircraft flew while in cloud ranged from 1.1 Km to 44.9 Km. A typical example of such a fly-through is shown in Fig. 1, where on May 2 the DC-8, flying at about 40,000 ft., penetrated a wave cloud near Berthoud, CO. This "Berthoud cloud" was a special case in that a second NASA Ames aircraft, the high-altitude ER-2, flew over the same portion of the cloud, and remotely measured cloud properties. In addition, there was a AVHRR satellite overpass that also permitted remote retrievals.

IWC measured by the PVM in these clouds was about 25% larger than IWC measured by the CVI. Figure 1 shows a typical comparison of IWC measured by the two probes. It also shows that the CVI IWC exhibits a hysteresis effect, because after the DC-8 passed through the upwind edge of the cloud at 73,755 s UT (universal time), the CVI continued to show a decreasing amount of IWC for about three minutes. This tail in the CVI IWC is caused by water vapor being flushed out of the instrument where

Copyright 1998 by the American Geophysical Union.

Paper number 97GL03310.
0094-8534/98/97GL-03310\$05.00

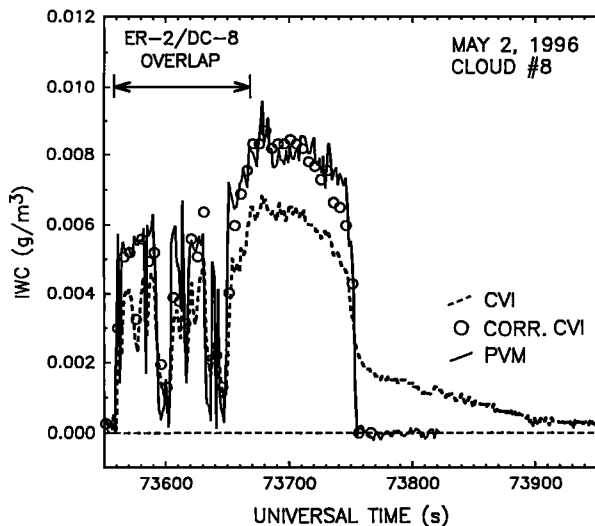


Figure 1. Ice water content (IWC) measured in the Berthoud wave cloud with the CVI and PVM probes; data points (o) show corrected CVI data. The DC-8 aircraft penetrated the cloud while the ER-2 aircraft flew over the same cloud in the overlap.

it had been adsorbed by the probe's interior surfaces during the evaporation of ice crystals while in cloud. If we make the assumption that the loss of vapor to the interior surfaces in the CVI is proportional to the magnitude of IWC measured by the CVI while in cloud, we can retrieve the "actual" CVI IWC in cloud by calculating the vapor loss from the amount of IWC in the hysteresis tail. This procedure was applied to the CVI data for all the cloud passes, and it resulted in a mean ratio of $IWC(PVM)/IWC(CVI) = 0.99$ with a standard deviation of 0.151. These statistics result in an uncertainty of this ratio of ± 0.07 (95% confidence level). This uncertainty compares favorably with the published accuracy estimates for the two probes: $\pm 10\%$ for the CVI (Twohy et al., 1997), and $\pm 5\%$ to $\pm 10\%$ for the PVM measuring spherical particles (Gerber et al., 1994.)

Figure 2 summarizes IWC measured by the two probes in twenty of the wave clouds penetrated on the two days. Here IWC has been converted to horizontal IWP (ice water path), which is simply the integral of $IWC \times \text{time of flight through cloud} \times \text{DC-8 speed}$.

An additional source of error for the PVM IWC measurements comes from the fact that the shape of the ice crystals in the wave clouds was not perfectly spherical as shown by the VIPS instrument (Heymsfield and McFarquhar, 1996) on the DC-8. An average ice crystal axial ratio of 1.32 was calculated from the VIPS data for the Berthoud cloud, assuming that the ice crystal were oblate spheroids. This leads to an approximately 5.2% overestimate in the IWC measured by the PVM, given that the response of the PVM is proportional to the cube of the randomly-oriented crystals' geometric cross section (Gerber et al., 1995) which can be estimated for the given axial ratio from Asano and Sato (1980). Similar calculations

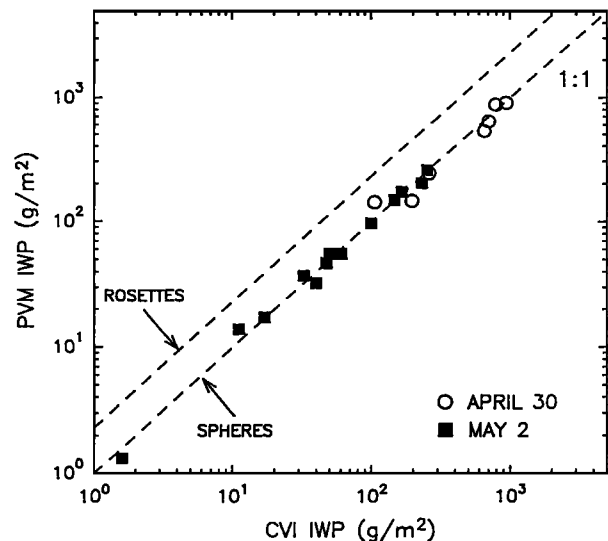


Figure 2. Horizontal ice water path (IWP) measured by CVI and PVM for all wave-cloud passes on the two dates indicated. Dashed lines show the influence of two ice-crystal shapes on PVM measurements.

done for rosettes and added to Fig. 2 show that the predicted large overestimate of PVM IWC for rosettes is inconsistent with the good agreement between PVM and CVI measurements that suggests the presence of sphere-like crystals in these wave clouds.

Additional evidence for the validity of the CVI and PVM IWC measurements can be found by comparing the measurements to estimates of the range of IWC values expected in the two sets of wave clouds; see Fig. 3. The

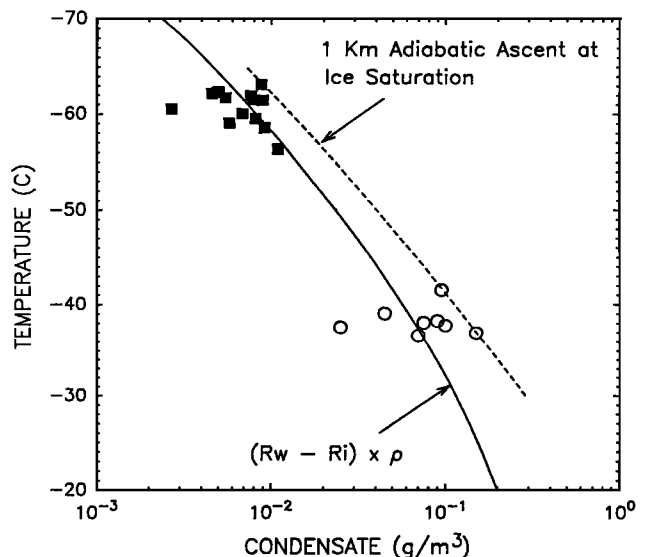


Figure 3. Calculated condensate (solid line) for the difference in water and ice mixing ratios R times air density, compared to average IWC measured by the CVI or PVM for the two wave-cloud cases shown in Fig. 2. The dashed line is the condensate amount when a 1-Km adiabatic ascent in the clouds is included.

lower limit of the range is estimated by taking the difference between the water vapor saturation mixing ratio (R_w) and the water vapor saturation mixing ratio over ice (R_i), and multiplying this difference by the air density (ρ); this condensate (IWC) forms after solution droplets freeze by homogeneous nucleation near the leading edge of these cold wave clouds, see Heymsfield and Miloshevich (1993, 1995). An upper limit is estimated by including an ice-adiabatic ascent in the clouds of 1 Km (dashed line). The proximity of the estimates and measurements in Fig. 3 suggests that the measured IWC values are reasonable. Figure 3 further suggests that the formation of ice in these cold wave clouds depends strongly on the change in the water vapor mixing ratio after initial ice formation, and that a first-order estimate of the average IWC is simply proportional to the difference of the mixing ratios for ice and water for a given cloud temperature.

Ice Crystal Size

Both PVM and CVI have the capability of estimating a characteristic ice crystal size. The CVI measures the number of CN (condensation nuclei) remaining after the ice crystals are evaporated. Under the assumption that one nuclei corresponds to one ice crystal, the crystal concentration N is determined. This is a reasonable assumption, because the counterflow of clean nitrogen at the entrance nozzle of the CVI permits the entrance of crystals only greater than about $3\text{-}\mu\text{m}$ radius, while preventing the entrance of the smaller ambient nuclei. Given IWC and N , permits the calculation of R_v (mean volume radius) of the ice crystals. This was done for the ER-2/DC-8 overlap region for the Berthoud cloud in Fig. 1, and yielded a value of $R_v = 8.1\text{-}\mu\text{m}$ radius. This value of R_v is approximately equivalent to $R_e = 8.9\text{-}\mu\text{m}$ radius, given that the shape of the average size distribution of the crystals determined from the VIPS data for this cloud is nearly lognormal and has a geometric standard deviation of 1.37.

The PVM has a second channel that measures PSA (projected surface area) of the ice crystals. This, along with the measured IWC yields R_e , because $R_e = (30,000/\rho_{ice}) \times (IWC/PSA)$, where $\rho_{ice} = .917\text{ g cm}^{-3}$. Figure 4 shows a plot of individual data points for PSA and IWC measured for the ER-2/DC-8 overlap region of Fig. 1. The slope of the best-fit straight line in Fig. 4 can be used to calculate the mean value of $R_e = 5.8\text{-}\mu\text{m}$ radius. Small ambient nuclei and particles do not affect this value of R_e , because the PVM has a predicted lower size cutoff in its response of about $2\text{-}\mu\text{m}$ radius. The $5.8\text{-}\mu\text{m}$ value is approximately 30% smaller than R_e measured by the CVI for the same cloud. Other estimates of R_e determined by remote sensing of the same cloud (described elsewhere in this issue) give an average $R_e = 7\text{ }\mu\text{m}$ from ER-2 measurements (Ackerman et al., 1998), and $R_e = 9\text{ }\mu\text{m}$ from the AVHRR satellite retrieval (Young et al., 1998.)

Figure 4 also illustrates a characteristic typical of the wave clouds on both April 30 and May 2: The values of R_e measured by the PVM as a function of time in the wave

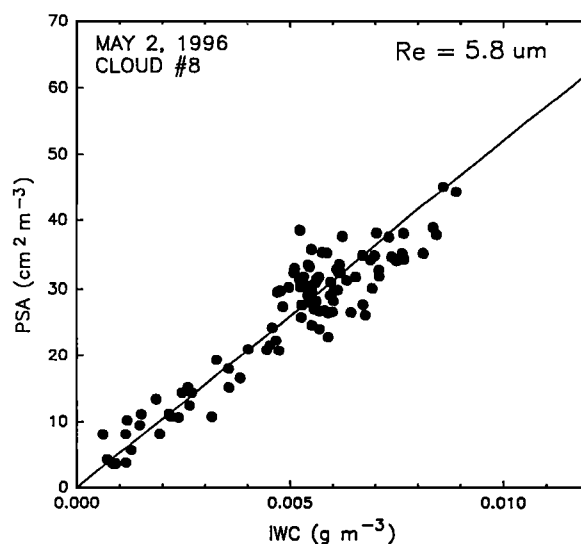


Figure 4. IWC and PSA (projected surface area) measured by the PVM for the two aircraft overlap region shown in Fig. 1. The slope of the line is inversely proportional to R_e (effective radius of the crystals.)

clouds vary over a relatively small range. The spectral dispersion of R_e (standard deviation of R_e divided by the mean of R_e) is 0.18 for the Berthoud cloud, as well as for the well-formed wave clouds west and north of Denver; and the dispersion of R_e for the April-30 clouds is .16. This relatively small variation in a characteristic size of the ice crystals agrees with earlier measurements (Heymsfield and Miloshevich, 1995) and more recent modeling (Jensen et al., 1998; DeMott et al., 1998) of crystal size in wave clouds with temperatures colder than about $-37\text{ }^{\circ}\text{C}$. At those temperatures homogeneous nucleation of ice, and principal growth of ice crystals near the leading edge of the wave clouds, appear to contribute to the lack of strong variability in cloud microphysics.

Ice crystal concentration

The concentration of ice crystals, N , can be estimated from PVM measurements of IWC and R_e given the crystals' lognormal shape of their size distribution which we assume applies to all the clouds. The PVM and CVI compare as follows: The warmer clouds found on April 30 show better relative agreement between average N measured by CVI (24 cm^{-3}) and PVM (35 cm^{-3}) than N measured by the CVI (3.0 cm^{-3}) and PVM (9.2 cm^{-3}) on May 2: The latter difference can not be presently explained; however, we speculate that it may be related to the uncertainty in the cutoff size for small ice crystals that differs for each probe, and to the expectation that smaller crystals predominated on May 2.

Conclusions

1) The comparison of CVI and PVM IWC and IWP measurements in the SUCCESS wave clouds shows

agreement within about +/- 15% after a correction is made to the CVI data for a hysteresis effect, and after an estimate is made of error in the PVM data due to the observed small deviation of the ice crystals from spherical shape. This agreement enhances the confidence in the use of each instrument, and suggests that the CVI will provide accurate measurements in ambient ice clouds containing all kinds of ice crystal habits and shapes, because it measures independently of those two parameters.

2) The comparison of IWC measured by the CVI and PVM with IWC predicted for the April-30 and May-2 wave clouds gives reasonable agreement, and suggests that a first order estimate of IWC in these cold wave clouds can be found by calculating the difference between the saturation vapor mixing ratios of water and ice at a known cloud temperature.

3) Re measured by the CVI and PVM and retrieved from ER-2 (Ackerman et al., 1997) and AVHRR (Young et al., 1997) remote sensing agreed within 30% for the Berthoud cloud.

4) The magnitude of IWC, the mean ice crystal size, and lack of strong variability of this size in the April-30 and May-2 wave clouds are consistent with the earlier findings in similar cold wave clouds with temperatures of -37 °C and colder (Heymsfield and Miloshevich, 1995.)

Acknowledgments. We thank the NASA Ames technical staff for fabricating the fairing for the PVM, without which the PVM could not have been deployed on the DC-8. We acknowledge the excellent scientific management of the SUCCESS DC-8 effort in Salina, KS. This work was partially supported by the NASA SASS Program.

References

- Asano, S., and M. Sato, Light scattering by randomly oriented spheroidal particles, *Appl. Opt.*, **19**, 962-974, 1980.
- Ackerman, S.A., C.C. Moeller, K.I. Stabala, H. Gerber, L.E. Gumley, and W.P. Menzel, Effective microphysical properties of different cloud types derived from an infrared retrieval algorithm, *Geophys. Res. Lett.*, this issue, 1998.
- DeMott, P.J., D.C. Rogers, S.M. Kreidenweis, and Y. Chen, The role of heterogeneous freezing nucleation in upper tropospheric clouds: Some inferences from SUCCESS, *Geophys. Res. Lett.*, this issue, 1998.
- Gerber, H., B.G. Arends, and A.S. Ackerman, New microphysics sensor for aircraft use, *Atmos. Res.*, **32**, 235-252, 1994.
- Gerber, H., P.J. DeMott, and D.C. Rogers, Laboratory investigation of direct measurement of ice water content, ice surface area, and effective radius of ice crystals using a laser-diffraction instrument, *Final Report No. 1*, NAS2-1426, NASA Ames, Moffett Field, CA, 1995.
- Heymsfield, A.J., and L.M. Miloshevich, Homogeneous ice nucleation and supercooled liquid water in orographic wave clouds, *J. Atmos. Sci.*, **50**, 2335-2353, 1993.
- Heymsfield, A.J., and L.M. Miloshevich, Relative humidity and temperature influences on cirrus formation and evolution: Observations from wave clouds and FIRE II, *J. Atmos. Sci.*, **52**, 4302-4326, 1995.
- Heymsfield, A.J., and G.M. Farquhar, High albedo of cirrus in the tropical Pacific warm pool: microphysical interpretations from CEPEX and from Kwajalein, Marshall Islands, *J. Atmos. Sci.*, **53**, 2424-2451, 1996.
- Jensen, E.J., O.B. Toon, A. Tabazadeh, G.S. Satche, B.E. Anderson, K.R. Chan, D. Baumgardner, C.H. Twohy, B. Gandrud, A.J. Heymsfield, J. Hallett, and B.L. Gary, Ice nucleation processes in upper tropospheric wave-clouds observed during SUCCESS, *Geophys. Res. Lett.*, this issue, 1998.
- Noone, K.J., J.A. Ogren, J. Heintzenberg, R.J. Charlson, and D.S. Covert, Design and calibration of a counterflow virtual impactor for sampling atmospheric fog and cloud droplets, *Aerosol Sci. Tech.*, **8**, 235-244, 1988.
- Ström, J., and J. Heintzenberg, Water vapor, condensed water, and crystal concentration in orographically influenced cirrus clouds. *J. Atmos. Sci.*, **51**, 2368-2383, 1994.
- Ström, J., B. Struss, T. Anderson, J. Heintzenberg, and P. Wendling, Measurement and modeling study of young cirrus clouds: Part 1, measurements, *Proc. 11th Int. Conf. on Clouds and Precipitation*, Zurich, Switzerland, 138-141, August 1996.
- Twohy, C.H., A.J. Schanot, and W.A. Cooper, Measurement of condensed water content in liquid and ice clouds using an airborne counterflow virtual impactor, *J. Atmos. Oceanic Technol.*, **14**, 197-202, 1997.
- Young, D.F., P. Minnis, D. Baumgardner, and H. Gerber, Comparisons of in-situ and satellite-derived cloud properties during SUCCESS, *Geophys. Res. Lett.*, this issue, 1998.

(Received July 1, 1997; revised October 28, 1997; accepted November 11, 1997.)